Hybrid Energy Harvesting Wireless Systems: Performance Evaluation and Benchmarking

Shilpa Rao and Neelesh B. Mehta, *Senior Member, IEEE*

***Abstract*—Energy harvesting (EH) is an attractive and green solution to the problem of limited lifetime of wireless sensor networks (WSNs). Unlike a conventional node that dies once it runs out of energy, an EH node harvests energy from the environment and replenishes its rechargeable battery. We investigate a new class of hybrid networks that comprise both EH and conventional nodes and differ from conventional and all-EH WSNs. We propose two new and insightful performance criteria called k-outage duration and n-transmission duration to evaluate these networks. They overcome the pitfalls associated with defining lifetime, which arise because the EH nodes never die but can occasionally run out of energy, and capture the dynamic time evolution, which occurs because the conventional nodes irreversibly drain their batteries. They also account for the inability of the nodes to transmit data due to insufficient battery energy and channel fading. We prove two computationally efficient novel bounds for evaluating these criteria. Our results characterize the effect of the number of EH and conventional nodes and channel fading statistics on these criteria. Further, given a total cost constraint, we determine the conventional and EH node mixture in the network that optimizes these criteria.**

***Index Terms*—Energy harvesting, wireless sensor networks, lifetime, fading, outage, Markov chain, bounds.**

I. Introduction

Wireless sensor networks (WSNs) are increasingly being deployed for industrial, health, aerospace, environmental monitoring, and control applications [2]. In several deployment scenarios, it is cumbersome or expensive to run cables to power the sensor nodes. Therefore, these nodes consume energy from their pre-charged batteries for their operations. Over time, a node drains out its battery and dies. Eventually, the network itself fails to meet its sensing objective.

Improving network lifetime is, therefore, an important objective of WSN design. Depending on the service provided by the WSN and its network topology, different definitions of lifetime have been used [3]. In many papers, e.g., [4], [5], the death of the first node in the WSN is defined as lifetime. This definition is pessimistic because the other nodes in the network may still be capable of sensing and sending data. In [6], lifetime is defined as the death of a pre-specified fraction of nodes. However, the above definitions are based purely on the battery energies of the nodes, and do not account for the failures in sending the sensed data to a fusion node (FN) due to channel fading. In [7], [8], network lifetime is defined in the terms of the number of nodes that run out of energy and the number of communication failures that occurred between the sensor node and the FN. Other definitions of lifetime are based on sensing coverage [9], connectivity of the nodes to the FN [10], and coverage and connectivity [11]. However, [10], [11] employ a deterministic path loss model without fading.

Energy harvesting (EH) sensor nodes, which replenish the energy they consume by harvesting it from the environment and storing it in their batteries, provide a promising and green alternative to tackle the vexing problem of prolonging lifetime [12]–[15]. However, the energy harvesting process can be sporadic. Further, an EH node needs additional circuitry to harvest, store, and provide a regulated supply of the harnessed energy to its battery or super-capacitor [16]. Hence, it is likely to be more expensive than a simpler conventional node, which comes equipped with a pre-charged, non-rechargeable battery.

Given the above challenges, hybrid WSNs, which comprise of a mixture of EH nodes and conventional nodes, are likely. Upgradation of the legacy WSNs, in which conventional nodes are gradually replaced by EH nodes, also naturally leads to hybrid WSNs. Even a WSN consisting entirely of EH nodes behaves as a hybrid network when some of the EH nodes cannot harvest energy over a prolonged period of time.

A. Similarities/Differences with Conventional and All-EH WSNs

A hybrid WSN is similar, yet different from both conventional and all-EH WSNs, which consist only of EH nodes. As its conventional nodes irreversibly drain out their batteries over time, it is more like a conventional WSN than an all-EH WSN. However, as its EH nodes that became inactive due to lack of sufficient energy can harvest energy and become active later, it is more like an all-EH WSN than a conventional WSN.

In order to evaluate a hybrid network, one needs consistent performance criteria that can handle the volatility of the conventional nodes and the vitality of the EH nodes. This is a fundamental and challenging problem because conventional and all-EH WSNs have typically been evaluated using very disparate performance criteria. Existing lifetime definitions based on the death of the nodes are ill-suited for evaluating the hybrid network due to the presence of the EH nodes. At the same time, performance criteria based on steady state analysis such as active/inactive cycles, which are typically applied to all-EH

Manuscript received May 31, 2013; revised October 24, 2013, February 22, 2014, and April 15, 2014; accepted June 9, 2014. Date of publication June 19, 2014; date of current version September 8, 2014. This work was supported in part by a research grant from ANRC. This paper was presented in part at the IEEE Wireless Communications and Networking Conference (WCNC), Shanghai, China, April 2013. The associate editor coordinating the review of this paper and approving it for publication was P. Wang.

The authors are with the Department of Electrical Communication Engineering, Indian Institute of Science (IISc), Bangalore 560 012, India (e-mail: devashilpa@gmail.com; nbmehta@ece.iisc.ernet.in).

Digital Object Identifier 10.1109/TWC.2014.2331978

WSNs, fail to capture the dynamic evolution of the hybrid network and the contributions of the conventional nodes.

B. Contributions

We introduce two performance criteria, namely, *k-outage duration* and *n-transmission duration*, to evaluate the longevity and utility of a hybrid WSN. They overcome several of the aforementioned challenges.

The k-outage duration is defined as the average time required for k outages to occur in the WSN, where an outage is an event in which data does not reach the FN either due to lack of battery energy for transmission or due to the communication failures caused by channel fading. It is inspired by the definition of network lifetime [7], [8]. In a monitor and control application, in which the FN receives data from the sensors and applies appropriate controls thereafter, the FN can potentially fail to apply the optimal control when an outage occurs. The k-outage duration is indicative of the time until which the number of suboptimal controls applied fall in an acceptable range. In sensing critical applications, k will be small, while in routine monitoring applications, k will be large.

The n-transmission duration is an alternate, but related, performance measure that is defined as the average time needed for n measurements to reach the FN. Its applications are complementary to the k-outage duration. For example, in WSNs employed for parameter estimation in which the nodes send a measured parameter to the FN [17], it indicates how quickly the network can estimate the parameter, with n being the minimum number of measurements required for sufficient accuracy. It is also directly applicable to an all-EH network.

Our second contribution is the analysis of k-outage and n-transmission durations for a time-slotted hybrid WSN with a star topology.[1] The star topology is widely considered in the study of both conventional [8], [18] and all-EH WSNs [13], [15] and is a basic building block in WSNs. The practical IEEE 802.15.4 standard for WSNs supports the star topology [19]. We observe that computing these performance criteria is computationally challenging and memory intensive even with a small number of nodes in the system. To circumvent this challenge, we propose two hypothetical systems by grouping the nodes of the hybrid WSN and use them to develop two novel low-complexity upper bounds on the k-outage duration and two lower bounds on the n-transmission duration. These bounds use an innovative coupling between the channel fading, energy harvesting, and transmission processes of the hypothetical systems and the hybrid WSN. Extensive numerical results that study the effect of the number of conventional and EH nodes in the hybrid system are presented, and they empirically verify that our bounds are tight. We show that increasing the number of EH nodes has a markedly different effect on the system performance than increasing the number of conventional nodes. Finally, we apply the analytical tools developed to study a cost-constrained hybrid WSN deployment.

[1]Estimation and detection problems are not precluded by our model. However, the granularity of the information conveyed is not captured. Our approach, which focuses on how often information reaches the FN, has also been used in [7], [8].

C. Performance Criteria for Hybrid WSNs: A Discussion

The k-outage and n-transmission durations are suitable for evaluating hybrid WSNs as they bridge the gap between the disparate performance criteria used for conventional and all-EH WSNs. They capture the vitality of the EH nodes and the volatility of the conventional nodes. They account for channel and battery energy variations. They can also be applied to conventional WSNs and all-EH WSNs. They enable these different networks to be compared with each other, and help assess the benefits of EH nodes.

However, they are not without their shortcomings. Ideally, the performance evaluation of the WSN would be based on whether the FN can fuse the sensed data with sufficient accuracy and on how much time it requires for doing this. However, this makes the problem formulation very specific to the sensing and quantization rules, fusion rules, and communication protocols used by the system. Further, given the various performance criteria that have been explored for conventional WSNs, it does not seem possible to come up with an all-encompassing, yet tractable criterion for evaluating hybrid WSNs. In fact, even the definition of outage is specific to the system being considered.

D. Outline and Notation

The system model is developed in Section II. In Sections III and IV, we analyze the k-outage duration and the n-transmission duration, respectively. Numerical results in Section V are followed by our conclusions in Section VI.

We use the following notation henceforth. The probability of an event A is denoted by $\Pr(A)$. For a random variable (RV) X, its expected value is denoted by $\mathbb{E}[X]$ and its expected value conditioned on event A is denoted by $\mathbb{E}[X|A]$. The indicator function for an event A is denoted by $1_{\{A\}}$; it equals 1 if A occurs and is 0 otherwise. $\mathbf{v}^T$ denotes the transpose of the vector $\mathbf{v}$. For $b < a$, the sum $\sum_{i=a}^{b}$ is identically 0. The all-ones vector of size $n \times 1$ is denoted by $\mathbf{1}_n$. The set of non-negative integers is denoted by $\mathbb{Z}^+$. And, $\lfloor \cdot \rfloor$ denotes the floor function.

II. Hybrid WSN System Model

As shown in Fig. 1, we consider a hybrid WSN that has M_C conventional nodes, M_E EH nodes, and an FN. Each conventional node has a non-rechargeable battery with an initial energy of B_0. Each EH node's rechargeable battery can store a maximum of $B_{\max}^E$ units of energy. To be fair in comparing conventional and EH nodes, we assume that the battery of each EH node has a pre-charge energy of B_0.

Time is divided into slots of duration T_{slot}, where T_{slot} is less than or equal to the coherence interval. Let $h_i^C(t)$ and $h_j^E(t)$ denote the frequency-flat channel power gains of the ith conventional node and the jth EH node, respectively, in the tth time slot. For analytical tractability, $h_i^C(t)$ and $h_j^E(t)$ are assumed to be independent and identically distributed (i.i.d.),

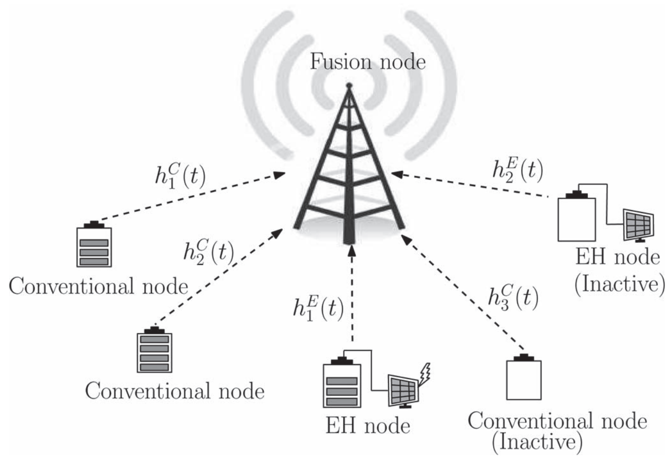

Fig. 1. Illustration of a hybrid WSN consisting of $M_E = 2$ EH nodes and $M_C = 3$ conventional nodes that transmit data to the FN over time-varying wireless links that undergo fading.

for $t \geq 1$, $1 \leq i \leq M_C$, and $1 \leq j \leq M_E$ [20]. Let γ_0 denote the mean channel power gain.

Energy Harvesting Model: The energy harvesting process of an EH node is modeled as a Bernoulli injection process. Such a model arises in switch-type [21] and vibrational [22] energy harvesters. It has been used in the literature [12], [23] because it captures the randomness in the harvested energy while also being tractable. An EH node harvests E_h units of energy in a slot with probability ρ, independently of other EH nodes. We note that the model in which the average energy harvested by the nodes is identical has been used in the EH literature [13], [15] in order to ensure tractability and gain valuable insights. The energy harvested in a slot is available for transmission in the next slot [6]. For tractability, B_0 is assumed to be an integer multiple of $E_h : B_0 = uE_h$, where $u \in \mathbb{Z}^+$. Similarly, $B_{\max}^E = dE_h$, where $d \in \mathbb{Z}^+$.

Transmission Scheme: A node that has sufficient battery energy to transmit with E_{tx} energy and whose channel power gain exceeds the threshold γ_{th} is called an *active* node. Here, γ_{th} depends on the modulation and coding scheme used by the node to transmit its sensed data to the FN, and is a system parameter. Such a fixed transmit power model has also been used in literature [15], [24] as it simplifies the power amplifier design, which is particularly relevant to lower complexity sensor nodes [24], [25]. Among the active nodes, the node with the largest battery energy is opportunistically selected to transmit in the time slot [8], [26]. If no node is active in a slot, then no transmission takes place in that slot and an outage occurs. Hence, in any slot at the most one node transmits.

Such opportunistic selection can be implemented using distributed algorithms, which work as follows. Each node has a preference number called its metric, which depends on its local parameters. In our system, the node's battery energy and channel gain to the FN determine its metric. The goal is to find the node with the highest metric. Two proficient selection algorithms are: *i) Timer based algorithm* [8], [26], [27]: In it, every node sets a timer value based on its metric and starts counting the timer down. The higher the metric, the lower the timer value. The node whose timer expires first transmits. Thus, the node with the highest metric transmits first. *ii) Splitting based algorithm* [28], [29]: Time is divided into mini-slots. A node transmits its packet in a mini-slot if its metric lies between a lower and an upper threshold. If the slot goes idle or a collision occurs, then the thresholds are accordingly updated for the next mini-slot. The process continues until a successful transmission occurs.

These selection algorithms are fast, distributed, scalable [27], [29] and energy-efficient [28]. The nodes operate on the basis of their local information. We, therefore, do not model the time and energy overhead of selection. The energy cost of sensing and data processing is neglected as radio transmission is often the dominant consumer of energy [12], [26]. For tractability, we set E_{tx} to be an integer multiple of $E_h : E_{\text{tx}} = lE_h$, where $l \in \mathbb{Z}^+$.

System Evolution: The transmission and harvesting process start from time slot $t = 1$. In time slot t, let $\mathcal{X}_i^C(t)$ be the event that the ith conventional node transmits, $\mathcal{X}_j^E(t)$ be the event that the jth EH node transmits, and $\mathcal{H}_j^E(t)$ be the event that the jth EH node harvests energy.

For the ith conventional node, the battery state $B_i^C(t+1)$ at the beginning of time slot $t+1$ evolves as

$$B_i^C(t+1) = B_i^C(t) - 1_{\{\mathcal{X}_i^C(t)\}} E_{\text{tx}}. \tag{1}$$

For the jth EH node, the battery state $B_j^E(t+1)$ at the beginning of time slot $t+1$ evolves as

$$B_j^E(t+1) = B_j^E(t) - 1_{\{\mathcal{X}_j^E(t)\}} E_{\text{tx}} + 1_{\{\mathcal{H}_j^E(t)\}} E_h. \tag{2}$$

Let $O(t)$ and $T(t)$ denote the number of outages and the number of transmissions, respectively, in the network at the end of time slot t. Clearly, $O(0) = 0$ and $T(0) = 0$. Let the RVs $\mathcal{T}_k$ and $\beth_n$ denote the time in slots required for k outages and n transmissions, respectively, to occur.

III. k-Outage Duration Analysis

At the beginning of time slot $t \geq 1$, the state $\mathbf{S}(t)$ of the network considering the battery energies of all the nodes and the number of outages can be represented as

$$\mathbf{S}(t) = \big(B_1^C(t), B_2^C(t), \ldots, B_{M_C}^C(t), \\ B_1^E(t), B_2^E(t), \ldots, B_{M_E}^E(t), O(t-1)\big). \tag{3}$$

$\{\mathbf{S}(t), t \geq 1\}$ is an absorbing discrete time Markov chain (DTMC). It is absorbing because once k outages occur, how the system evolves thereafter is no longer of interest.

The number of states in the state space of this DTMC is $(k+1)(u+1)^{M_C}(d+1)^{M_E}$, which is exponential in both M_C and M_E. This occurs because the battery energies of the nodes are coupled. Analyzing such a high dimensional Markov chain is computationally challenging and memory intensive. For example, even with $M_E = 2$, $M_C = 2$, $E_{\text{tx}} = 3E_h$, and $B_{\max}^E = 15E_{\text{tx}}$, the number of states exceeds a million. Therefore, alternative analytical approaches are essential. To this end, we present two novel upper bounds for $\mathbb{E}[\mathcal{T}_k]$ that have much lower computational complexity and, thus, effectively circumvent the problem. Henceforth, we shall refer to the system described above as the *original system*.

A. Single Pooled Battery (SP) System

In this hypothetical system, there is just one node called an *SP node* that transmits data to the FN. Its battery energy at the beginning of time slot t is denoted by $B_{\mathrm{SP}}(t)$. At the beginning of time slot 1, which we shall refer to as start-up, $B_{\mathrm{SP}}(1) = (M_C + M_E)B_0$, which is the total battery energy of all the nodes in the original system. The battery capacity of the SP node is the sum of the battery capacities of all nodes in the original system, and equals $b_{\mathrm{cap}}E_h$, where $b_{\mathrm{cap}} = uM_C + dM_E$.

As in the original system, each time slot is of length T_{slot}. We define the channel power gain $h_{\mathrm{SP}}(t)$ seen by the SP node in the tth time slot to be the maximum of the channel power gains seen by all the nodes in the original system in that slot:

$$h_{\mathrm{SP}}(t) = \max\left\{h_1^C(t), h_2^C(t), \ldots, h_{M_C}^C(t), h_1^E(t), h_2^E(t), \ldots, h_{M_E}^E(t)\right\}. \quad (4)$$

The energy harvested by the SP node in time slot t is the sum of the energies harvested by all the EH nodes in the original system in that slot; it equals $\sum_{j=1}^{M_E} 1_{\{\mathcal{H}_j^E(t)\}}E_h$. The SP node transmits in a slot t if it is active, i.e., if $B_{\mathrm{SP}}(t) \geq E_{\mathrm{tx}}$ and $h_{\mathrm{SP}}(t) \geq \gamma_{\mathrm{th}}$. Thus, the channel gains and the energy harvested by the SP node are both coupled to the original system.

1) SP System Based Upper Bound: Let $\mathbb{E}[\mathcal{T}_k^{\mathrm{SP}}]$ denote the k-outage duration of the SP system. The following result connects the k-outage durations of the original and SP systems.

Theorem 1: The k-outage duration of the original system is upper bounded by that of the SP system

$$\mathbb{E}[\mathcal{T}_k] \leq \mathbb{E}\left[\mathcal{T}_k^{\mathrm{SP}}\right]. \quad (5)$$

Proof: The proof is relegated to Appendix A. It turns out to be quite intricate because the effect of both the energy harvesting and energy consumption processes on the battery energies of the nodes and outages need to be accounted for. This also depends on the channel fading processes of all the nodes in the system. ■

2) Analysis of $\mathbb{E}[\mathcal{T}_k^{\mathrm{SP}}]$: Let $O_{\mathrm{SP}}(t)$ denote the number of outages that have occurred in the SP system at the end of time slot t. Clearly, $O_{\mathrm{SP}}(0) = 0$. The state of the SP system at the beginning of time slot t, which is analogous to $\mathbf{S}(t)$ in the original system, is

$$\mathbf{S}_{\mathrm{SP}}(t) = (B_{\mathrm{SP}}(t), O_{\mathrm{SP}}(t-1)).$$

Then, $\{\mathbf{S}_{\mathrm{SP}}(t), t \geq 1\}$ is a DTMC that takes values in the state space $\mathcal{S}_{\mathrm{SP}} \cup \mathcal{A}_{\mathrm{SP}}$, where

$$\mathcal{S}_{\mathrm{SP}} = \{(sE_h, o) : 0 \leq s \leq b_{\mathrm{cap}}, 0 \leq o \leq k-1\}, \quad (6)$$

$$\mathcal{A}_{\mathrm{SP}} = \{(sE_h, k) : 0 \leq s \leq b_{\mathrm{cap}}\}. \quad (7)$$

Here, $\mathcal{A}_{\mathrm{SP}}$ is the set of absorbing states of the DTMC, in which k outages have occurred, and $\mathcal{S}_{\mathrm{SP}}$ is the set of all the other non-absorbing states. *While the original system is a DTMC of dimension $M_C + M_E + 1$, the SP system is only a two-dimensional DTMC.*

The probability of moving from state (wE_h, x) to state $(w'E_h, x')$, where (wE_h, x) and $(w'E_h, x') \in \mathcal{S}_{\mathrm{SP}} \cup \mathcal{A}_{\mathrm{SP}}$, is represented by $p_{(w,x),(w',x')}$. The transition probability matrix $\mathbf{P}_k^{\mathrm{SP}}$ of the DTMC is given in Appendix B. Let the restriction of $\mathbf{P}_k^{\mathrm{SP}}$ on $\mathcal{S}_{\mathrm{SP}}$ be denoted by $\mathbf{Z}_k^{\mathrm{SP}}$. Now, $p_{(w,x),(w',x')}$ is the $(x(uM_C + dM_E + 1) + w + 1)$th row and $(x'(uM_C + dM_E + 1) + w' + 1)$th column element of $\mathbf{Z}_k^{\mathrm{SP}}$. Let $\mathbb{E}[\mathcal{T}_k^{\mathrm{SP}}|(w,x)]$ denote the k-outage duration of the SP system given that it starts from state $(wE_h, x) \in \mathcal{S}_{\mathrm{SP}}$ and let

$$\mathbf{v}^{\mathrm{SP}} = \left(\mathbb{E}\left[\mathcal{T}_k^{\mathrm{SP}}|(0,0)\right], \mathbb{E}\left[\mathcal{T}_k^{\mathrm{SP}}|(1,0)\right], \ldots, \mathbb{E}\left[\mathcal{T}_k^{\mathrm{SP}}|(uM_C + dM_E, k-1)\right]\right)^T, \quad (8)$$

be a $k(uM_C + dM_E + 1) \times 1$ vector of k-outage durations given that the DTMC starts from different states in $\mathcal{S}_{\mathrm{SP}}$.

As shown in Appendix C, $\mathbb{E}[\mathcal{T}_k^{\mathrm{SP}}]$ is given by

$$\mathbb{E}\left[\mathcal{T}_k^{\mathrm{SP}}\right] = \mathbb{E}\left[\mathcal{T}_k^{\mathrm{SP}}|\left(u\left(M_C + M_E\right), 0\right)\right]. \quad (9)$$

It is the $(u(M_C + M_E) + 1)$th element of $\mathbf{v}^{\mathrm{SP}}$, which simplifies to

$$\mathbf{v}^{\mathrm{SP}} = \left(\mathbf{I}_k^{\mathrm{SP}} - \mathbf{Z}_k^{\mathrm{SP}}\right)^{-1} \mathbf{1}_{k(uM_C + dM_E + 1)} \quad (10)$$

where $\mathbf{I}_k^{\mathrm{SP}}$ is an identity matrix of the same size as $\mathbf{Z}_k^{\mathrm{SP}}$.

3) Special Case With Only Conventional Nodes: If the network has only M_C conventional nodes and if $E_{\mathrm{tx}} = E_h$, then $\mathbb{E}[\mathcal{T}_k^{\mathrm{SP}}]$ can be written in a closed form as follows.

Theorem 2: The k-outage duration of the SP system when the original network consists of entirely conventional nodes and $E_{\mathrm{tx}} = E_h$ is given by

$$\mathbb{E}\left[\mathcal{T}_k^{\mathrm{SP}}\right] = (k + uM_C) - (1-\zeta)^k \times \sum_{a=0}^{uM_C - 1} (uM_C - a)\binom{k+a-1}{a}\zeta^a, \quad (11)$$

where ζ is the probability that $h_{\mathrm{SP}}(t)$ is at least γ_{th}.

Proof: The proof is given in Appendix D. ■

B. Dual Pooled Battery (DP) System

In this alternate hypothetical *DP system*, there are two nodes called *conventional pooled battery (CDP) node* and *EH pooled battery (EDP) node* that have data to transmit to the FN. As before, each time slot is of duration T_{slot}. At start-up, the battery energy of the CDP node is $M_C B_0$, which is the sum of the battery energies at start-up of all the conventional nodes in the original system. In time slot t, the channel power gains of the CDP and EDP nodes are the maximum of the channel power gains of the conventional nodes and the maximum of the channel power gains of the EH nodes in the original system, respectively. The EDP node has infinite energy in its battery in any time slot. When both the EDP and CDP nodes are active, the former is chosen for transmission. In a slot, an outage occurs only if the CDP and EDP nodes cannot transmit.

1) DP System Based Upper Bound: Let $\mathbb{E}[\mathcal{T}_k^{\mathrm{DP}}]$ be the average time required for k outages to occur in the DP system. The following key result connects the k-outage durations of the DP system and the original system.

Theorem 3: The k-outage duration of the DP system upper bounds that of the original system

$$\mathbb{E}[\mathcal{T}_k] \leq \mathbb{E}[\mathcal{T}_k^{\mathrm{DP}}]. \tag{12}$$

Proof: The proof is relegated to Appendix E. ■

We shall henceforth refer to the bounds based on the SP and DP systems as the SP and DP bounds, respectively. These bounds hold for any probability distribution of the channel power gains seen by the nodes and for any energy harvesting process. Intuitively, when the average energy harvested per slot by an EH node in the original system exceeds the average transmission energy per slot, the battery energy of the SP node increases with time, and outages due lack of battery energy in the conventional nodes do not get captured by it. However, in the DP system, the CDP node continues to track the drain in the battery energy of the conventional nodes. Hence, in this regime, the DP bound in (12) is tighter than the SP bound in (5). Here, the diversity in selecting the active node with the highest channel gain is also is captured more effectively by the DP system. Similarly, when the EH nodes harvest lesser energy, the SP bound is tighter.

We know from Theorems 1 and 3 that $\mathbb{E}[\mathcal{T}_k] \leq \mathbb{E}[\mathcal{T}_k^{\mathrm{SP}}]$ and $\mathbb{E}[\mathcal{T}_k] \leq \mathbb{E}[\mathcal{T}_k^{\mathrm{DP}}]$. Thus, combining the two, we get the following tighter upper bound:

$$\mathbb{E}[\mathcal{T}_k] \leq \min\left\{\mathbb{E}\left[\mathcal{T}_k^{\mathrm{SP}}\right], \mathbb{E}\left[\mathcal{T}_k^{\mathrm{DP}}\right]\right\}. \tag{13}$$

2) Analysis of $\mathbb{E}[\mathcal{T}_k^{\mathrm{DP}}]$: Let $B_{\mathrm{CDP}}(t)$ denote the battery energy of the CDP node at the beginning of time slot t. The number of outages in the DP system at the end of time slot t is denoted by $O_{\mathrm{DP}}(t)$. Clearly, $O_{\mathrm{DP}}(0) = 0$. The state of the DP system at the beginning of time slot t considering the CDP node's battery energy and the number of outages is given by

$$\mathbf{S}_{\mathrm{DP}}(t) = \left(B_{\mathrm{CDP}}(t), O_{\mathrm{DP}}(t-1)\right).$$

Note that the battery energy of the EDP node need not be tracked since it can transmit in any time slot so long as its channel power gain exceeds γ_{th}. We see that $\{\mathbf{S}_{\mathrm{DP}}(t), t \geq 1\}$ is a DTMC with state space $\mathcal{S}_{\mathrm{DP}} \cup \mathcal{A}_{\mathrm{DP}}$, where

$$\mathcal{S}_{\mathrm{DP}} = \left\{(sE_h, o) : 0 \leq s \leq uM_C, 0 \leq o \leq k-1\right\}, \tag{14}$$

$$\mathcal{A}_{\mathrm{DP}} = \left\{(sE_h, k) : 0 \leq s \leq uM_C\right\}. \tag{15}$$

Here, $\mathcal{A}_{\mathrm{DP}}$ and $\mathcal{S}_{\mathrm{DP}}$ are the sets of absorbing and non-absorbing states, respectively, of the DP system. Hence, analyzing the k-outage duration of the DP system also involves dealing with a much simpler two-dimensional DTMC. Its state transition probability matrix $\mathbf{P}_k^{\mathrm{DP}}$ is given in Appendix F.

Let $\mathbf{Z}_k^{\mathrm{DP}}$ be the restriction of $\mathbf{P}_k^{\mathrm{DP}}$ on $\mathcal{S}_{\mathrm{DP}}$. Then, the probability $q_{(w,x),(w',x')}$ of moving from state (wE_h, x) to $(w'E_h, x')$ is the $(x(uM_C+1)+w+1)$th row and $(x'(uM_C+1)+w'+1)$th column element of $\mathbf{Z}_k^{\mathrm{DP}}$. The k-outage duration of the DP system, given that it starts from state $(wE_h, x) \in \mathcal{S}_{\mathrm{DP}}$, is denoted by $\mathbb{E}[\mathcal{T}_k^{\mathrm{DP}}|(w,x)]$. Let

$$\mathbf{v}^{\mathrm{DP}} = \left(\mathbb{E}\left[\mathcal{T}_k^{\mathrm{DP}}|(0,0)\right], \mathbb{E}\left[\mathcal{T}_k^{\mathrm{DP}}|(1,0)\right], \ldots, \mathbb{E}\left[\mathcal{T}_k^{\mathrm{DP}}|\left(uM_C, k-1\right)\right]\right)^T, \tag{16}$$

be a $k(uM_C+1) \times 1$ vector.

The k-outage duration of the DP system is then given by

$$\mathbb{E}\left[\mathcal{T}_k^{\mathrm{DP}}\right] = \mathbb{E}\left[\mathcal{T}_k^{\mathrm{DP}}|\left(uM_C, 0\right)\right],$$

where $\mathbb{E}[\mathcal{T}_k^{\mathrm{DP}}|(uM_C, 0)]$ is the (uM_C+1)th element of the vector $\mathbf{v}^{\mathrm{DP}}$, and

$$\mathbf{v}^{\mathrm{DP}} = \left(\mathbf{I}_k^{\mathrm{DP}} - \mathbf{Z}_k^{\mathrm{DP}}\right)^{-1} \mathbf{1}_{k(uM_C+1)}. \tag{17}$$

Here, $\mathbf{I}_k^{\mathrm{DP}}$ is an identity matrix of the same size as $\mathbf{Z}_k^{\mathrm{DP}}$. The proof is along lines similar to Appendix C.

IV. n-Transmission Duration Analysis

We now analyze the n-transmission duration of the hybrid network. To calculate it, at any time $t \geq 1$, we need to track the battery energies of all nodes in the original system and the number of transmissions that have occurred thus far. Hence, the state of the network at the beginning of time slot $t \geq 1$, $\tilde{\mathbf{S}}(t)$, can be represented as

$$\tilde{\mathbf{S}}(t) = \left(B_1^C(t), B_2^C(t), \ldots, B_{M_C}^C(t), B_1^E(t), B_2^E(t), \ldots, B_{M_E}^E(t), T(t-1)\right). \tag{18}$$

$\{\tilde{\mathbf{S}}(t), t \geq 1\}$ is again an $(M_C + M_E + 1)$-dimensional DTMC with $(n+1)(u+1)^{M_C}(d+1)^{M_E}$ states. The large state space of this DTMC again makes it difficult to evaluate $\mathbb{E}[\beth_n]$ even when the number of nodes is small.

We present two computationally simpler lower bounds for $\mathbb{E}[\beth_n]$. Let $\mathbb{E}[\beth_n^{\mathrm{SP}}]$ and $\mathbb{E}[\beth_n^{\mathrm{DP}}]$ denote the n-transmission durations of the SP and DP systems, respectively.

Theorem 4: The n-transmission durations of the SP and DP systems each lower bound the n-transmission duration of the original system

$$\mathbb{E}[\beth_n] \geq \mathbb{E}\left[\beth_n^{\mathrm{SP}}\right], \tag{19}$$

$$\mathbb{E}[\beth_n] \geq \mathbb{E}\left[\beth_n^{\mathrm{DP}}\right]. \tag{20}$$

Proof: The proof is relegated to Appendix G. ■

The following tighter lower bound follows:

$$\mathbb{E}[\beth_n] \geq \max\left\{\mathbb{E}\left[\beth_n^{\mathrm{SP}}\right], \mathbb{E}\left[\beth_n^{\mathrm{DP}}\right]\right\}. \tag{21}$$

We now evaluate $\mathbb{E}[\beth_n^{\mathrm{SP}}]$ and $\mathbb{E}[\beth_n^{\mathrm{DP}}]$, which, as before, shall be referred to as the SP and DP bounds, respectively.

A. Evaluating $\mathbb{E}[\beth_n^{\mathrm{SP}}]$

Let $T_{\mathrm{SP}}(t)$ denote the number of transmissions in the SP system at the end of time slot t. Clearly, $T_{\mathrm{SP}}(0) = 0$. The state of the SP system at the beginning of time slot t considering the

SP node's battery energy and the number of transmissions by the SP node is $\tilde{\mathbf{S}}_{\mathrm{SP}}(t) = (B_{\mathrm{SP}}(t), T_{\mathrm{SP}}(t-1))$. Then, $\{\tilde{\mathbf{S}}_{\mathrm{SP}}(t), t \geq 1\}$ is a DTMC with state space $\tilde{\mathcal{S}}_{\mathrm{SP}} \cup \tilde{\mathcal{A}}_{\mathrm{SP}}$, where

$$\tilde{\mathcal{S}}_{\mathrm{SP}} = \{(sE_h, \chi) : 0 \leq s \leq b_{\mathrm{cap}}, 0 \leq \chi \leq n-1\}, \quad (22)$$

$$\tilde{\mathcal{A}}_{\mathrm{SP}} = \{(sE_h, n) : 0 \leq s \leq b_{\mathrm{cap}}\}. \quad (23)$$

Here, $\tilde{\mathcal{A}}_{\mathrm{SP}}$ is the set of absorbing states of the DTMC in which n transmissions have occurred. Hence, $\mathbb{E}[\beth_n^{\mathrm{SP}}]$ can be analyzed using a much simpler, two-dimensional DTMC, as follows.

Let the probability of moving from state (wE_h, x) to state $(w'E_h, x')$ be represented by $\tilde{p}_{(w,x),(w',x')}$. Let $\tilde{\mathbf{P}}_n^{\mathrm{SP}}$ denote the transition probability matrix of the DTMC. It is given in Appendix H. Let its restriction on $\tilde{\mathcal{S}}_{\mathrm{SP}}$ be denoted by $\tilde{\mathbf{Z}}_n^{\mathrm{SP}}$. Now, $\tilde{p}_{(w,x),(w',x')}$ is the $(x(uM_C + dM_E + 1) + w + 1)$th row and $(x'(uM_C + dM_E + 1) + w' + 1)$th column element of $\tilde{\mathbf{Z}}_n^{\mathrm{SP}}$. It can be shown that $\mathbb{E}[\beth_n^{\mathrm{SP}}]$ is the $(u(M_C + M_E) + 1)$th element of the $n(uM_C + dM_E + 1) \times 1$ vector $\tilde{\mathbf{v}}^{\mathrm{SP}}$, and

$$\tilde{\mathbf{v}}^{\mathrm{SP}} = \left(\tilde{\mathbf{I}}_n^{\mathrm{SP}} - \tilde{\mathbf{Z}}_n^{\mathrm{SP}}\right)^{-1} \mathbf{1}_{n(uM_C + dM_E + 1)}, \quad (24)$$

where $\tilde{\mathbf{I}}_n^{\mathrm{SP}}$ is an identity matrix of the same size as $\tilde{\mathbf{Z}}_n^{\mathrm{SP}}$.

B. Evaluating $\mathbb{E}[\beth_n^{\mathrm{DP}}]$

Let $T_{\mathrm{DP}}(t)$ denote the number of transmissions in the DP system at the end of time slot t. Clearly, $T_{\mathrm{DP}}(0) = 0$. The state of the DP system at the beginning of time slot t considering the battery energy of the CDP node and all the transmissions by the DP system is given by $\tilde{\mathbf{S}}_{\mathrm{DP}}(t) = (B_{\mathrm{CDP}}(t), T_{\mathrm{DP}}(t-1))$. Thus, $\{\tilde{\mathbf{S}}_{\mathrm{DP}}(t), t \geq 1\}$ is a DTMC with state space $\tilde{\mathcal{S}}_{\mathrm{DP}} \cup \tilde{\mathcal{A}}_{\mathrm{DP}}$, where $\tilde{\mathcal{S}}_{\mathrm{DP}}$ and $\tilde{\mathcal{A}}_{\mathrm{DP}}$ are the set of its non-absorbing and absorbing states, respectively, and are given by

$$\tilde{\mathcal{S}}_{\mathrm{DP}} = \{(sE_h, \chi) : 0 \leq s \leq uM_C, 0 \leq \chi \leq n-1\}, \quad (25)$$

$$\tilde{\mathcal{A}}_{\mathrm{DP}} = \{(sE_h, n) : 0 \leq s \leq uM_C\}. \quad (26)$$

Along lines similar to Section IV-A, $\mathbb{E}[\beth_n^{\mathrm{DP}}]$ can be easily evaluated. The steps are not shown here to conserve space.

C. Computational Complexity

By analyzing the DTMC $\mathbf{S}(t)$ in (3), it can be shown that $k(u+1)^{M_C}(d+1)^{M_E}$ linearly independent equations need to be solved to evaluate the k-outage duration of the original system. On the other hand, as seen from (10) and (17), only $k(uM_C + dM_E + 1)$ and $k(uM_C + 1)$ linearly independent equations have to be solved to calculate the k-outage durations of the SP and DP systems, respectively. Solving a system of m linear equations entails a computational complexity of $\mathcal{O}(m^{2.376})$ [30]. Thus, computing the SP and DP bounds entails a significantly lower computational complexity. Similar complexity reductions occur for the n-transmission duration as well.

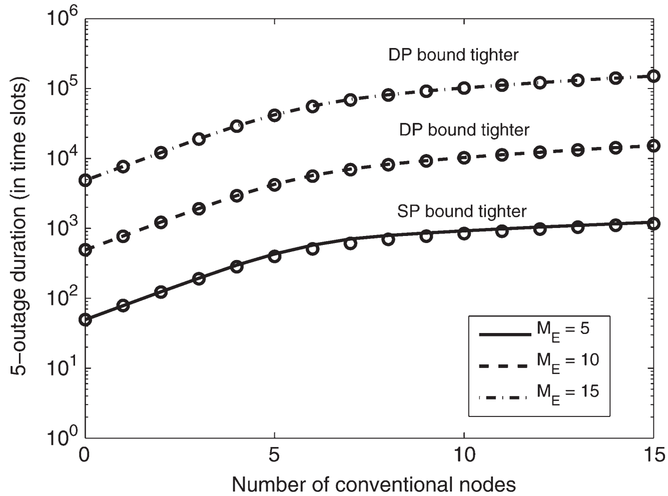

Fig. 2. 5-outage duration as a function of M_C for different M_E ($\rho = 0.5$, $E_{\mathrm{tx}}/E_h = 3$, and $\gamma_{\mathrm{th}} = 1$). Simulation results are shown using the marker ○. The lines depict the bound in (13).

V. Numerical Results and Cost Effective Hybrid WSN Design

We now study the behavior of the original system using Monte Carlo simulations that average over 10^5 sample paths, and evaluate the efficacy of the bounds. Unless mentioned otherwise, we assume Rayleigh fading and set $\gamma_0 = 1$, $B_0/E_{\mathrm{tx}} = 10$, and $B_{\max}/E_{\mathrm{tx}} = 15$.

A. k-Outage Duration

Fig. 2 plots the 5-outage duration measured from simulations and its upper bound in (13) as a function of M_C for different values of M_E.[2] As M_E increases, the 5-outage duration increases because the odds that at least one node sees a channel power gain that is greater than γ_{th} increase and the batteries of the conventional nodes get drained less often. Similarly, as M_C increases, the 5-outage duration increases. For smaller M_E, the SP bound is tighter because the total energy harvested by the system is low, which makes it the dominant cause for outages. This energy shortage is captured well by the SP system since it undergoes the same energy injection process. For larger M_E, the DP bound is tighter because the odds that the EH nodes transmit are higher. This behavior is effectively captured by the EDP node of the DP system. We see that the bounds continue to be tight as the number of nodes increases.

Fig. 3 plots the 5-outage duration measured from simulations and its upper bound in (13) as a function of M_E for different M_C. As M_C increases, the 5-outage duration increases because more nodes are available in the system to transmit data to the FN. The maximum error between the bound and the simulations is 7% and the average error is 2%. Thus, the proposed bound is again tight. Unlike Fig. 2, in which the 5-outage duration increases more rapidly as M_E increases, here, the increase is marginal as M_C increases.

[2] Even efficient C language programs for simulating the original system with a larger number of nodes had high, multi-day execution times. This is because of the exponential increase in the number of states in the DTMCs.

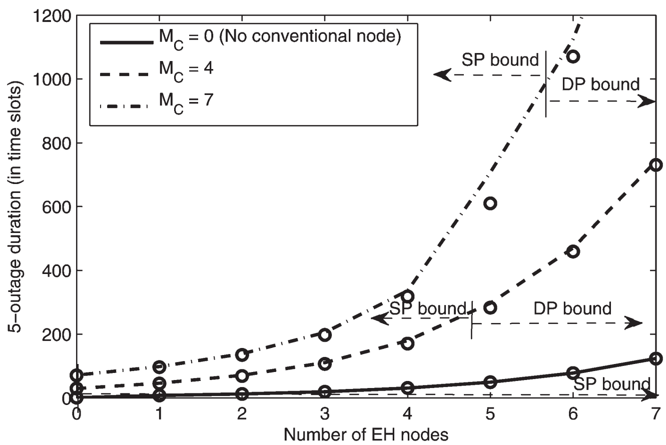

Fig. 3. 5-outage duration as a function of M_E for different M_C ($\rho = 0.5$, $E_{\rm tx}/E_h = 3$, and $\gamma_{\rm th} = 1$). Simulation results are shown using the marker ○. The lines depict the bound in (13).

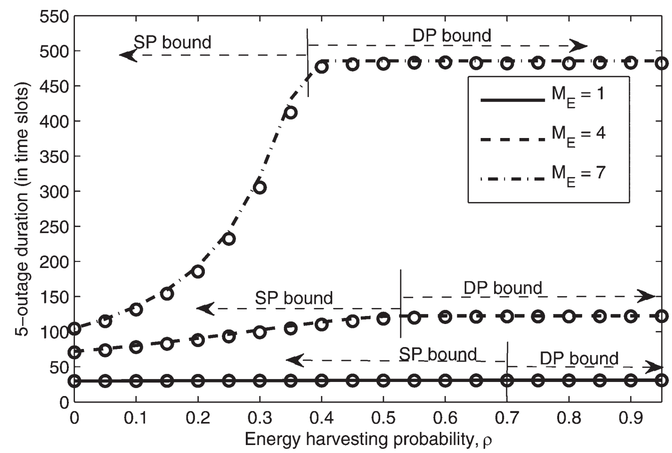

Fig. 5. 5-outage duration as a function of energy harvesting probability ($M_C = 3$, $E_{\rm tx}/E_h = 3$, and $\gamma_{\rm th} = 1$). Simulation results are shown using the marker ○. The lines depict the bound in (13).

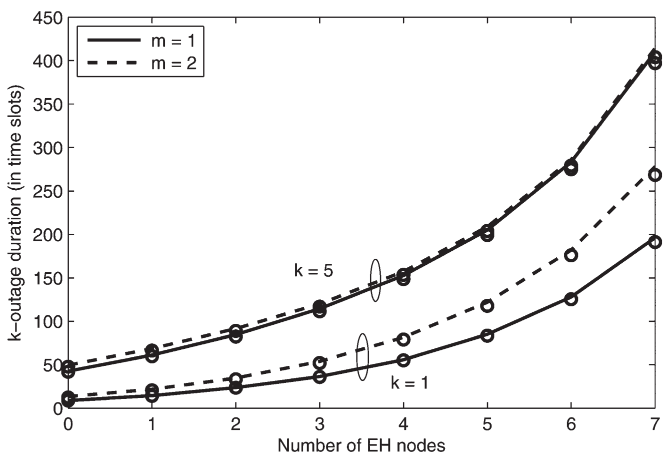

Fig. 4. Effect of k and channel fading statistics on the k-outage duration ($M_C = 5, \rho = 0.1, E_{\rm tx}/E_h = 1$, and $\gamma_{\rm th} = 1$). Simulation results are shown using the marker ○. The lines depict the bound in (13).

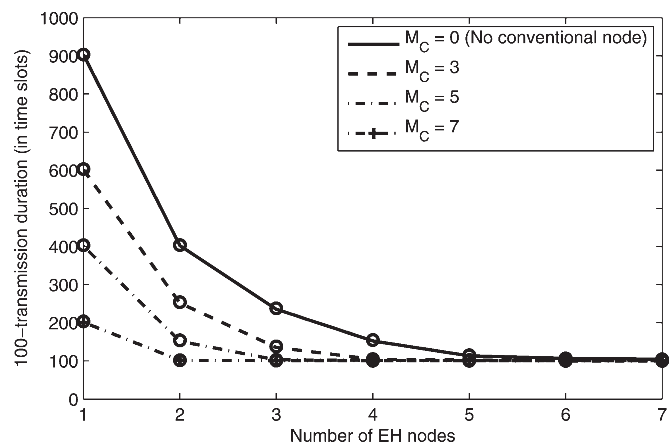

Fig. 6. 100-transmission duration as a function of M_E for different M_C ($\rho = 0.1$, $E_{\rm tx}/E_h = 1$, and $\gamma_{\rm th} = 1$). Simulation results are shown using the marker ○. The lines depict the bound in (21).

Fig. 4 evaluates the effect of channel fading statistics and k by showing results for Nakagami-m fading. It plots the k-outage duration as a function of M_E for $k = 1$ and $k = 5$, and for $m = 1$ (Rayleigh fading) and $m = 2$. Both simulation results and the bound in (13) are shown. As k increases, the k-outage duration increases, which is intuitive. However, it turns out that it saturates for larger k (figure not shown). This is because for large k, the odds that the conventional nodes drain out their batteries by the time k outages occur is high. Now, the number of EH nodes primarily determine the k-outage duration. Also, as m increases, the k-outage duration increases because, for the same mean power gain, the odds that the channel power gains of the nodes exceed $\gamma_{\rm th}$ increases. The bound is tight and captures the effect of the channel statistics.

Fig. 5 shows the 5-outage duration as a function of the energy harvesting probability ρ for different values of M_E. As ρ increases, the 5-outage duration increases and later saturates. This is because for larger ρ, the channel fades and not lack of energy are primarily responsible for the occurrence of outages. Also demarcated in the figure are the regimes in which the SP and DP bounds are tighter. For smaller ρ, the SP bound is tighter because the EH nodes in the system are energy starved, while for larger ρ, the reverse is true.

Note: In general, the tightness of the bounds depends on B_0. The bounds are tight for moderate to large values of B_0, but are relatively loose for very small B_0. However, the latter regime is of limited interest since a practical deployment is unlikely to be energy-starved right from its inception.

B. n-Transmission Duration

Fig. 6 plots the 100-transmission duration measured from simulations and its lower bound in (21) as a function of M_E for different M_C.[3] The maximum error between the lower bound and the simulations is 2%. Thus, the bound is again tight. As M_E or M_C increase, the 100-transmission duration decreases for reasons similar to those in Section V-A.

[3]When $M_E = 0$, the system cannot achieve 100 transmissions because the total energy in the system can support only $10M_C$ transmissions even when M_C is as large as 7. Therefore, results for $M_E = 0$ are not shown.

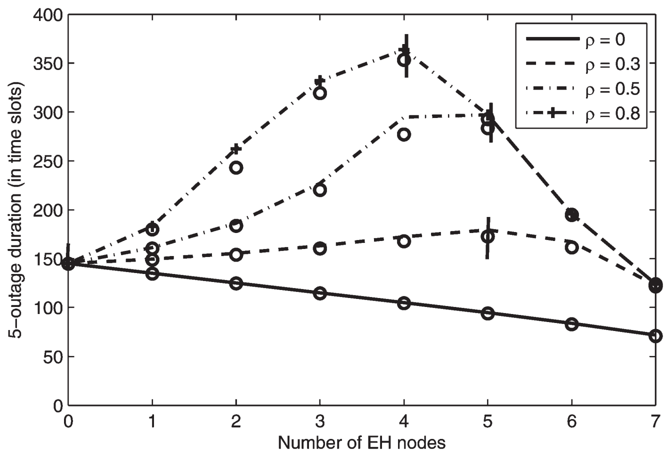

Fig. 7. Effect of ρ on M_E^* for the 5-outage duration ($E_{\rm tx}/E_h = 3$, $\gamma_{\rm th} = 1$, $c_T = 14$, $c_c = 1$, and $c_E = 2$). Simulation results are shown using marker ○. The lines depict the bound in (13). For every ρ, M_E^* is indicated by a short vertical line.

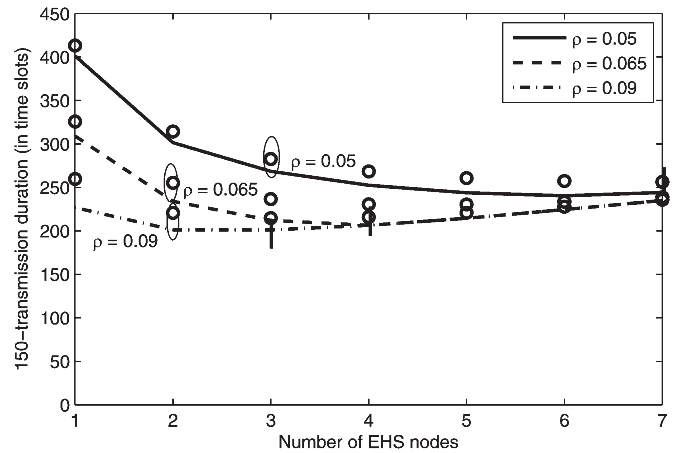

Fig. 8. Effect of ρ on $M_E^\dagger$ for the 150-transmission duration ($E_{\rm tx}/E_h = 1$, $\gamma_{\rm th} = 2$, $c_T = 14$, $c_c = 1$, and $c_E = 2$). Simulation results are shown using marker ○. The lines depict the bound in (21). For every ρ, $M_E^\dagger$ is indicated by a short vertical line.

C. Cost-Effective WSN Design

We now determine the optimal deployment of a hybrid WSN that is subject to a total cost constraint. Let c_C and c_E be the cost of one conventional node and one EH node, respectively, with $c_E \geq c_C$. Let c_T indicate the upper limit on the total cost for system deployment. Hence, the total network cost $c_C M_C + c_E M_E$ must be less than or equal to c_T.

Our first goal is to find the optimal values of M_C and M_E, denoted by M_C^* and M_E^*, respectively, that maximize the k-outage duration. We use the computationally simpler bounds derived in Section III, which the simulation results empirically indicate are tight everywhere, to determine M_C^* and M_E^*.[4] The optimization problem can be stated as:

$$(M_C^*, M_E^*) = \underset{(M_C, M_E)}{\arg\max}\ \min\left\{\mathbb{E}\left[\mathcal{T}_k^{\rm SP}\right], \mathbb{E}\left[\mathcal{T}_k^{\rm DP}\right]\right\}, \quad (27)$$

$$\text{s.t.} \quad c_T \geq c_C M_C + c_E M_E, \quad (28)$$

which is easily solved by an exhaustive search because of the low computational complexity of the bounds.

Fig. 7 plots the 5-outage duration as a function of M_E for different values of ρ. As M_E increases, the 5-outage duration increases initially because more energy is harvested. It then reaches a maximum and then decreases because the number of cheaper conventional nodes in the system decreases at a faster rate. This reduces the number of active nodes in the network, which increases the incidence of outages. For every ρ, the optimal M_C^* and M_E^* pair that maximizes the upper bound on $\mathbb{E}[\mathcal{T}_5]$ is also the one obtained from simulations. When ρ is very small, EH nodes do not improve the k-outage duration much. Therefore, the optimal configuration does not employ any of the more expensive EH nodes. As ρ increases, more EH nodes typically get employed in the network. Note that the optimal configuration obtained from the bounds is the same as that obtained from optimizing the original system using extensive Monte Carlo simulations.

Along similar lines as above, we now evaluate $\arg\min_{M_C, M_E} \max\{\mathbb{E}[\beth_n^{\rm SP}], \mathbb{E}[\beth_n^{\rm DP}]\}$ subject to the total cost constraint of (28). The optimal configuration, which is denoted by $M_C^\dagger$ and $M_E^\dagger$, is found numerically. Fig. 8 plots the 150-transmission duration obtained from simulations and its lower bound (cf. (21)) as a function of M_E for different values of ρ. As before, we see that the optimal value obtained from the bounds matches that obtained from the simulations. The optimal number of EH nodes decreases as ρ increases. This is because when ρ is small, having more EH nodes significantly increases the odds that at least one among them has enough energy to transmit.

VI. Conclusion

We studied a new class of hybrid networks that consist of both conventional and EH nodes, and is different from both conventional and all-EH WSNs. We proposed the use of the k-outage and n-transmission durations as performance criteria for evaluating and comparing such networks. They account for the effect of battery energies and communication failures due to channel fading on the performance of the WSN, and avoid the pitfalls associated with defining lifetime based or steady state based criteria. We developed two computationally simpler upper bounds for the k-outage duration and lower bounds for the n-transmission duration. Finally, we determined cost-effective hybrid deployments to optimize these two criteria.

Several interesting avenues for future research exist given the fundamental nature of the questions that arise in our study. These include more sophisticated models that use a mesh topology, power control, and physical layer diversity techniques. Another interesting avenue is the inclusion of temporal and spatial correlation in the channel fading and energy harvesting processes in the network.

[4]A more rigorous approach would be to analytically prove that the gap between $\mathbb{E}[\mathcal{T}_k]$ and $\mathbb{E}[\mathcal{T}_k^{\rm SP}]$ or $\mathbb{E}[\mathcal{T}_k^{\rm DP}]$ is small. However, this is extremely challenging because the battery evolutions of the nodes are coupled.

APPENDIX

A. Proof of Theorem 1

We compare the evolution of the original and SP systems in parallel for a given sample path of the energy harvesting and channel fading processes. The total energy provided to the SP node prior to time slot t is $(M_C + M_E)B_0 + \sum_{\tau=1}^{t-1}\sum_{j=1}^{M_E} 1_{\{\mathcal{H}_j^E(\tau)\}} E_h$. Since each transmission consumes energy $E_{\rm tx}$, the number of transmissions $T_{\rm SP}(t)$ by the SP node until the end of time slot t cannot exceed $T_{\max}(t)$, where

$$T_{\rm SP}(t) \leq T_{\max}(t) = \left\lfloor \left((M_C+M_E)B_0 + \sum_{\tau=1}^{t-1}\sum_{j=1}^{M_E} 1_{\{\mathcal{H}_j^E(\tau)\}} E_h \right) \frac{1}{E_{\rm tx}} \right\rfloor.$$

This follows because the numerator above is the sum of the SP node's initial battery energy and the total energy it harvests until the start of time slot t. By the same reasoning, the number of transmissions $T(t)$ by the original system by time t obeys the inequality $T(t) \leq T_{\max}(t)$.

Notice that $T(t)$ and $T_{\rm SP}(t)$ are monotonically non-decreasing functions of t. Further, in both systems, either a transmission or an outage occurs in every slot. Hence,

$$t = T_{\rm SP}(t) + O_{\rm SP}(t) = T(t) + O(t), \quad \text{for } t \geq 1. \tag{29}$$

The SP system evolves in one of the following two ways:

i) $T_{\rm SP}(t) < T_{\max}(t)$, *for all* $t \geq 1$: In this case, the energy in the SP node's battery in the beginning of slot t is at least

$$\begin{aligned}(T_{\max}(t) - T_{\rm SP}(t-1)) E_{\rm tx} &\geq (T_{\max}(t) - T_{\rm SP}(t)) E_{\rm tx}, \\ &\geq E_{\rm tx}.\end{aligned} \tag{30}$$

Since $h_{\rm SP}(t)$ is at least as good as the channel seen by the transmitting node in the original system, the SP node will transmit whenever a node in the original system transmits. Hence, $T_{\rm SP}(t) - T(t) \geq 0$, for $t \geq 1$. Using (29), we get

$$O(t) - O_{\rm SP}(t) = T_{\rm SP}(t) - T(t) \geq 0, \quad \text{for } t \geq 1. \tag{31}$$

ii) $T_{\rm SP}(t) = T_{\max}(t)$, *for* $t = t_0, t_1, t_2, \ldots$, *where* $t_0 < t_1 < t_2 < \cdots$, *and* $T_{\rm SP}(t) < T_{\max}(t)$, *otherwise*: Using (29), for $r \geq 0$, we get

$$\begin{aligned}O(t_r) - O_{\rm SP}(t_r) &= T_{\rm SP}(t_r) - T(t_r), \\ &= T_{\max}(t_r) - T(t_r) \geq 0.\end{aligned} \tag{32}$$

For $0 \leq t < t_0$, since $T_{\rm SP}(t) < T_{\max}(t)$, the reasoning in the previous case implies that $O(t) \geq O_{\rm SP}(t)$.

We will now prove that $O(t) \geq O_{\rm SP}(t)$, for $t_r < t < t_{r+1}$, for all $r \geq 0$. The following two cases can occur: a) $T_{\rm SP}(t_{r+1}) = T_{\rm SP}(t_r)$, or b) $T_{\rm SP}(t_{r+1}) > T_{\rm SP}(t_r)$.

a) *When* $T_{\rm SP}(t_r) = T_{\rm SP}(t_{r+1})$: This implies that $T_{\max}(t_r) = T_{\max}(t_{r+1})$. By the definition of $t_0, t_1, \ldots$, this can happen only when $t_{r+1} = t_r + 1$. Thus, there are no intermediate time slots that need to be covered, and we are done.

b) *When* $T_{\rm SP}(t_{r+1}) > T_{\rm SP}(t_r)$: Consider $r = 0$. If $t_1 = 1 + t_0$, then we are done. Else, in time slots $t_0 + 1 \leq t < t_1$, we know that $T_{\rm SP}(t) < T_{\max}(t)$. Then, in each of these slots, the battery energy in the SP node is lower bounded by

$$B_{\rm SP}(t) \geq (T_{\max}(t) - T_{\rm SP}(t-1)) E_{\rm tx} \geq E_{\rm tx},$$

where the last inequality follows because

$$T_{\rm SP}(t-1) \leq T_{\rm SP}(t) < T_{\max}(t).$$

Hence, using the same reasoning as before, the number of transmissions by the SP system in the time interval $t_0 + 1, \ldots, t_1 - 1$ is greater than or equal to that by the original system, i.e., $T(t) \leq T_{\rm SP}(t)$. Hence, from (29), we can again show that

$$O(t) - O_{\rm SP}(t) \geq 0, \quad \text{for} \quad t_0 + 1 \leq t < t_1.$$

Similarly, by induction, it can be shown that the same holds for any $1 + t_r \leq t < t_{r+1}$, for all $r \geq 1$. Hence,

$$O(t) \geq O_{\rm SP}(t), \quad \text{for} \quad t \geq 1. \tag{33}$$

Since $O(\mathcal{T}_k) = k$, this implies that $O_{\rm SP}(\mathcal{T}_k) \leq k$. Hence, $\mathcal{T}_k \leq \mathcal{T}_k^{\rm SP}$, which implies that $\mathbb{E}[\mathcal{T}_k] \leq \mathbb{E}[\mathcal{T}_k^{\rm SP}]$.

B. Transition Probability Matrix $\mathbf{P}_k^{\rm SP}$ of SP System

The probability $p_{(w,x),(w',x')}$ that the SP system moves from state (wE_h, x) to state $(w'E_h, x')$ is obtained as follows. Once the SP system is in an absorbing state, it remains there. Else, if $(wE_h, x) \notin \mathcal{A}_{\rm SP}$, then the following two cases arise.

i) SP Node Does Not Transmit: The outage count increases to $x + 1$. This happens if: a) The SP node has no energy for transmission, $B_{\rm SP}(t) < E_{\rm tx}$, or b) $h_{\rm SP}(t) < \gamma_{\rm th}$, which happens with probability $1 - \zeta$. For example, for Rayleigh fading, we have $\zeta = 1 - (1 - \exp(-(\gamma_{\rm th}/\gamma_0)))^{M_C+M_E}$.

Also, if yE_h energy is harvested, then $B_{\rm SP}(t)$ increases from wE_h to $(w + y)E_h$. This happens with probability σ_y, where

$$\sigma_y = \binom{M_E}{y} \rho^y (1-\rho)^{M_E - y}, \quad \text{for} \quad y \geq 0.$$

Therefore, $p_{(w,x),(w+y,x+1)}$, for $w + y < b_{\rm cap}$, is given by

$$p_{(w,x),(w+y,x+1)} = \begin{cases} \sigma_y, & wE_h < E_{\rm tx}, \\ (1-\zeta)\sigma_y, & wE_h \geq E_{\rm tx}. \end{cases} \tag{34}$$

The probability of moving from (wE_h, x) to $(b_{\rm cap}E_h, x + 1)$ is

$$p_{(w,x),(b_{\rm cap},x+1)} = \begin{cases} \sum_{y=b_{\rm cap}-w}^{M_E} \sigma_y, & wE_h < E_{\rm tx}, \\ (1-\zeta)\sum_{y=b_{\rm cap}-w}^{M_E} \sigma_y, & wE_h \geq E_{\rm tx}. \end{cases} \tag{35}$$

ii) SP Node Transmits: The SP node transmits if: a) It has sufficient battery energy, $B_{\rm SP}(t) \geq E_{\rm tx}$, and b) $h_{\rm SP}(t) \geq \gamma_{\rm th}$, which happens with probability ζ. Since a transmission has occurred, the outage count remains unchanged. After a transmission, the battery energy of the SP node is $(w - l + y)E_h$ with probability σ_y. Therefore, for $wE_h \geq E_{\rm tx}$ and

$(w-l+y)E_h < b_{\text{cap}}E_h,\ p_{(w,x),(w-l+y,x)} = \zeta\sigma_y$. Similarly, $p_{(w,x),(b_{\text{cap}},x)} = \zeta\sum_{y=b_{\text{cap}}-w+l}^{M_E}\sigma_y$. All other transition probabilities are 0.

C. Deriving $\mathbb{E}[\mathcal{T}_k^{\text{SP}}]$

When the SP system starts from the state $(wE_h, x) \in \mathcal{A}_{\text{SP}}$, k outages have already occurred. Hence, the time required for k outages to occur given that the SP system starts from state $(wE_h, x) \in \mathcal{A}_{\text{SP}}$ is zero. Therefore, the absorbing states need not be considered in the analysis.

If the system is in state $(wE_h, x) \in \mathcal{S}_{\text{SP}}$, it transits into the state $(w'E_h, x')$ in the next time slot with probability $p_{(w,x),(w',x')}$. Given the Markovian evolution of the SP system, the k-outage duration, given that the current state is $(wE_h, x) \in \mathcal{S}_{\text{SP}}$, is equal to

$$\mathbb{E}\left[\mathcal{T}_k^{\text{SP}} | (w,x)\right] = 1 + \sum_{w'=0}^{uM_C+dM_E}\sum_{x'=x}^{x+1}\mathbb{E}\left[\mathcal{T}_k^{\text{SP}} | (w',x')\right] \times p_{(w,x),(w',x')}. \quad (36)$$

Writing in terms of $\mathbf{v}^{\text{SP}}$, we get $(\mathbf{I}_k^{\text{SP}} - \mathbf{Z}_k^{\text{SP}})\mathbf{v}^{\text{SP}} = \mathbf{1}_{k(uM_C+dM_E+1)}$, from which (10) follows.[5]

D. Brief Proof of Theorem 2

Since no node harvests energy and $E_{\text{tx}} = E_h$, the transitions probabilities in Appendix B simplify as follows:

i) *SP Node Does Not Transmit*: The outage count increases by one and the battery level remains the same. Hence, $p_{(w,x),(w,x+1)} = 1$ when $w = 0$, and $p_{(w,x),(w,x+1)} = 1-\zeta$ when $w > 0$.

ii) *SP Node Transmits*: This happens only when the SP node has at least E_h energy and its channel power gain is at least γ_{th}. Therefore, $p_{(w,x),(w-1,x)} = \zeta$, for $w > 0$. All other transition probabilities are zero. With this, we can show using mathematical induction that for $1 \le r \le k$ and $0 \le g \le uM_C$,

$$\mathbb{E}\left[\mathcal{T}_k^{\text{SP}} | (g, k-r)\right] = (g+r) - (1-\zeta)^k \sum_{a=0}^{g-1}(g-a)\binom{g+a-1}{a}\zeta^a.$$

Substituting $(g, k-r) = (uM_C, 0)$ in this equation yields (11).

E. Proof of Theorem 3

Consider a sample path of the channel fading and energy harvesting processes. Let $T_C(t)$ and $T_E(t)$ denote the total transmissions by all the conventional nodes and by all the EH nodes, respectively, in the original system at the end of time slot t. Let $T'_C(t)$ and $T'_E(t)$ denote the number of transmissions by the CDP and EDP nodes, respectively, at the end of slot t. The CDP node has sufficient energy to transmit at most $T_{C_{\max}}$ packets each of energy E_{tx}, where $T_{C_{\max}} = \lfloor (M_C B_0)/E_{\text{tx}} \rfloor$. Hence, for $t \ge 1$, we know that $T'_C(t) \le T_{C_{\max}}$. Similarly, in the original system, $T_C(t) \le T_{C_{\max}}$, for $t \ge 1$. In both systems, either a transmission or an outage occurs in any slot. Hence,

$$t = T_C(t) + T_E(t) + O(t) = T'_C(t) + T'_E(t) + O_{\text{DP}}(t). \quad (37)$$

We first show the following intermediate result.

Claim 1: For $t \ge 1$, $T'_E(t) \ge T_E(t)$.

Proof: The EDP node is inactive if and only if the channel power gains of all the EH nodes in the original system are below γ_{th}. Thus, if at least one EH node is active in the original system, then the EDP node must also be active. By the design of the DP system, the EDP node transmits any time it is active. On the other hand, in the original network, none of the active EH nodes may be selected to transmit. Hence, the EDP node transmits at least as many times as the total number of times the EH nodes transmit in the original system.

Thus, $T'_E(t) \ge T_E(t)$, for $t \ge 1$. ■

The following two possible cases for $T'_C(t)$ arise:

i) $T'_C(t) < T_{C_{\max}}$: Since $T'_C(\tau) \le T'_C(t)$, for all $1 \le \tau \le t$, it follows that at the beginning of time slot $\tau \le t$, the CDP node's battery energy is

$$\left(T_{C_{\max}} - T'_C(\tau-1)\right)E_{\text{tx}} \ge \left(T_{C_{\max}} - T'_C(t)\right)E_{\text{tx}} \ge E_{\text{tx}}.$$

If at least one conventional node in the original system has a channel power gain that exceeds γ_{th} in time slot τ, then the channel power gain of the CDP node, which sees the maximum of the channel power gains of all the conventional nodes, also exceeds γ_{th}. Thus, the CDP node is active in time slot τ if at least one conventional node is active in the original system in that slot.

We already know from the proof of Claim 1 given above that the EDP node is active in slot τ if at least one EH node in the original system is active in this slot. Hence, if $T'_C(t) < T_{C_{\max}}$, then a transmission occurs in the DP system in all the slots $1, 2, \ldots, t$ in which a transmission occurs in the original system. Therefore, $O_{\text{DP}}(t) \le O(t)$ when $T'_C(t) < T_{C_{\max}}$.

ii) $T'_C(t) = T_{C_{\max}}$: From Claim 1 and (37), we get $T_{C_{\max}} + O_{\text{DP}}(t) \le T_C(t) + O(t)$. Rearranging the terms, we get $O(t) \ge O_{\text{DP}}(t) + (T_{C_{\max}} - T_C(t)) \ge O_{\text{DP}}(t)$. Hence, in both cases,

$$O_{\text{DP}}(t) \le O(t), \quad \text{for} \quad t \ge 1. \quad (38)$$

Now, along the lines of Appendix A, it easily follows that $\mathbb{E}[\mathcal{T}_k] \le \mathbb{E}[\mathcal{T}_k^{\text{DP}}]$.

F. Transition Probability Matrix $\mathbf{P}_k^{\text{DP}}$ of the DP System

Let ζ_C and ζ_E denote the probabilities that the channel power gain seen by a CDP and EDP node, respectively, exceed γ_{th}. Once the system enters $\mathcal{A}_{\text{DP}}$, it stays there. Else, the probability $q_{(w,x),(w',x')}$ that the DP system moves from (wE_h, x) to $(w'E_h, x')$ is obtained as follows.

[5] As long as all the states $(wE_h, x) \in \mathcal{S}_{\text{SP}}$ are transient, the matrix $(\mathbf{I}_k^{\text{SP}} - \mathbf{Z}_k^{\text{SP}})$ is invertible. If some state $(wE_h, x) \in \mathcal{S}_{\text{SP}}$ is absorbing, then (10) no longer holds and the k-outage duration is infinity.

i) *When* $(wE_h, x) \in \mathcal{S}_{\text{DP}}$ *and No Transmission Occurs in the System*: This happens when both the CDP and EDP nodes are inactive. The EDP node is inactive only if $h_{\text{EDP}}(t) < \gamma_{\text{th}}$, which happens with probability $1 - \zeta_E$. The CDP node is inactive if: a) $B_{\text{CDP}}(t) = wE_h < E_{\text{tx}}$, or b) $h_{\text{CDP}}(t) < \gamma_{\text{th}}$, which happens with probability $1 - \zeta_C$. In this case, the outage count increases by 1 and the energy of the CDP node does not change. Therefore, the next state is $(wE_h, x+1)$. Hence, for $0 \le x \le k-1$, we have

$$q_{(w,x),(w,x+1)} = \begin{cases} (1-\zeta_E)(1-\zeta_C), & wE_h \ge E_{\text{tx}}, \\ 1-\zeta_E, & wE_h < E_{\text{tx}}. \end{cases} \quad (39)$$

ii) *When* $(wE_h, x) \in \mathcal{S}_{\text{DP}}$ *and a Transmission Occurs*: The following two cases arise:

a) *EDP Node Transmits*: For this, the EDP node must be active, which happens with probability ζ_E. Thus, the battery energy of the CDP node does not change and the outage count stays the same. Since the system state does not change, we have $q_{(w,x),(w,x)} = \zeta_E$.

b) *CDP Node Transmits*: This happens only if the EDP node is inactive. This happens with probability $(1-\zeta_E)\zeta_C$. The energy of the CDP node decreases by E_{tx} and the outage count stays the same. Hence, the state changes from (wE_h, x) to $((w-l)E_h, x)$, and the transition probability is $q_{(w,x),(w-l,x)} = (1-\zeta_E)\zeta_C$, for $wE_h \ge E_{\text{tx}}$.

All other transition probabilities are 0.

G. Proof of Theorem 4

Consider a given sample path of the energy harvesting and channel fading processes. From (29) and (33), we already know that $T(t) \le T_{\text{SP}}(t)$, for $t \ge 1$. By definition,

$$T(\beth_n) = n. \quad (40)$$

Hence, $T_{\text{SP}}(\beth_n) \ge n$. This means that the number of transmissions by the SP node by time $\beth_n$ is greater than or equal to n. Therefore, $\beth_n^{\text{SP}} \le \beth_n$. This directly implies that $\mathbb{E}[\beth_n^{\text{SP}}] \le \mathbb{E}[\beth_n]$.

From the definition of $T_{\text{DP}}(t)$, we know that $T_{\text{DP}}(t) = T'_C(t) + T'_E(t)$, for $t \ge 1$. Similarly, $T(t) = T_C(t) + T_E(t)$, for $t \ge 1$. From (37) and (38) we know that $T_C(t) + T_E(t) \le T'_C(t) + T'_E(t)$. Thus, the above relationships together imply that $T(t) \le T_{\text{DP}}(t)$, which, in turn, implies that $T_{\text{DP}}(\beth_n) \ge n$. Hence, from (40), it follows that $\mathbb{E}[\beth_n] \ge \mathbb{E}[\beth_n^{\text{DP}}]$.

H. Transition Probability Matrix $\tilde{\mathbf{P}}_n^{\text{SP}}$ of the SP System

The transition probability $\tilde{p}_{(w,x),(w,',x')}$ from (wE_h, x) to $(w'E_h, x')$ is obtained as follows. Once the SP system enters $\tilde{\mathcal{A}}_{\text{SP}}$, it remains there. Else, if $(wE_h, x) \notin \tilde{\mathcal{A}}_{\text{SP}}$, then two cases arise:

i) *SP Node Does Not Transmit*: As in Appendix B, for $w + y < b_{\text{cap}}$, we can show that

$$\tilde{p}_{(w,x),(w+y,x)} = \begin{cases} \sigma_y, & wE_h < E_{\text{tx}}, \\ (1-\zeta)\sigma_y, & wE_h \ge E_{\text{tx}}, \end{cases} \quad (41)$$

and

$$\tilde{p}_{(w,x),(b_{\text{cap}},x)} = \begin{cases} \sum_{y=b_{\text{cap}}-w}^{M_E} \sigma_y, & wE_h < E_{\text{tx}}, \\ (1-\zeta)\sum_{y=b_{\text{cap}}-w}^{M_E} \sigma_y, & wE_h \ge E_{\text{tx}}. \end{cases} \quad (42)$$

ii) *SP Node Transmits*: For $wE_h \ge E_{\text{tx}}$ and $(w-l+y)E_h < b_{\text{cap}}E_h$, we have $\tilde{p}_{(w,x),(w-l+y,x+1)} = \zeta\sigma_y$. Similarly,

$$\tilde{p}_{(w,x),(b_{\text{cap}},x+1)} = \zeta \sum_{y=b_{\text{cap}}-w+l}^{M_E} \sigma_y, \quad \text{for } wE_h \ge E_{\text{tx}}.$$

All other transition probabilities are 0.

References

[1] S. Rao and N. B. Mehta, "Hybrid energy harvesting wireless systems: Performance evaluation and benchmarking," in *Proc. IEEE WCNC*, Apr. 2013, pp. 4244–4249.

[2] I. F. Akyildiz, T. Melodia, and K. R. Chowdury, "Wireless multimedia sensor networks: A survey," *IEEE Wireless Commun.*, vol. 14, no. 6, pp. 32–39, Dec. 2007.

[3] I. Dietrich and F. Dressler, "On the lifetime of wireless sensor networks," *ACM Trans. Sens. Netw.*, vol. 5, no. 1, pp. 1–39, Feb. 2009.

[4] R. Madan, S. Cui, S. Lal, and A. Goldsmith, "Cross-layer design for lifetime maximization in interference-limited wireless sensor networks," *IEEE Trans. Wireless Commun.*, vol. 5, no. 11, pp. 3142–3152, Nov. 2006.

[5] W. Wang, V. Srinivasan, and K. C. Chua, "Extending the lifetime of wireless sensor networks through mobile relays," *IEEE/ACM Trans. Netw.*, vol. 16, no. 5, pp. 1108–1120, May 2008.

[6] K. Ramachandran and B. Sikdar, "A population based approach to model the lifetime and energy distribution in battery constrained wireless sensor networks," *IEEE J. Sel. Areas Commun.*, vol. 28, no. 4, pp. 576–586, Apr. 2010.

[7] Y. Chen and Q. Zhao, "Maximizing the lifetime of sensor network using local information on channel state and residual energy," in *Proc. CISS*, Mar. 2005, pp. 1–5.

[8] K. Cohen and A. Leshem, "A time-varying opportunistic approach to lifetime maximization of wireless sensor networks," *IEEE Trans. Signal Process.*, vol. 58, no. 10, pp. 5307–5319, Oct. 2010.

[9] H. Zhang and J. Hou, "On the upper bound of α-lifetime for large sensor networks," *ACM Trans. Sens. Netw.*, vol. 1, no. 2, pp. 272–300, Nov. 2005.

[10] B. Cărbunar, A. Grama, J. Vitek, and O. Cărbunar, "Redundancy and coverage detection in sensor networks," *ACM Trans. Sens. Netw.*, vol. 2, no. 1, pp. 94–128, Feb. 2006.

[11] W. Mo, D. Qiao, and Z. Wang, "Mostly-sleeping wireless sensor networks: Connectivity, k-coverage, and α-lifetime," in *Proc. Allerton Conf. Commun., Control, Comput.*, Sep. 2005, pp. 886–895.

[12] J. Lei, R. Yates, and L. Greenstein, "A generic model for optimizing single-hop transmission policy of replenishable sensors," *IEEE Trans. Wireless Commun.*, vol. 8, no. 2, pp. 547–551, Feb. 2009.

[13] A. Seyedi and B. Sikdar, "Energy efficient transmission strategies for body sensor networks with energy harvesting," *IEEE Trans. Commun.*, vol. 58, no. 7, pp. 2116–2126, Jul. 2010.

[14] D. Niyato, E. Hossain, and A. Fallahi, "Sleep and wakeup strategies in solar-powered wireless sensor/mesh networks: Performance analysis and optimization," *IEEE Trans. Mobile Comput.*, vol. 6, no. 2, pp. 221–236, Feb. 2007.

[15] F. Iannello, O. Simeone, and U. Spagnolini, "Medium access control protocols for wireless sensor networks with energy harvesting," *IEEE Trans. Commun.*, vol. 60, no. 5, pp. 1381–1389, May 2012.

[16] S. Sudevalayam and P. Kulkarni, "Energy harvesting sensor nodes: Survey and implications," *IEEE Commun. Surveys Tuts.*, vol. 13, no. 3, pp. 443–461, 2011.

[17] O. Akan and I. Akyildiz, "Event-to-sink reliable transport in wireless sensor networks," *IEEE/ACM Trans. Netw.*, vol. 13, no. 5, pp. 1003–1016, Oct. 2005.

[18] Y. Chen, Q. Zhao, V. Krishnamurthy, and D. Djonin, "Transmission scheduling for optimizing sensor network lifetime: A stochastic shortest path approach," *IEEE Trans. Signal Process.*, vol. 55, no. 5, pp. 2294–2309, May 2007.

[19] *IEEE Standard for Local and Metropolitan Area Networks, IEEE Std 802.15.4e-2012 (Amendment to IEEE Std 802.15.4-2011)*, IEEE Std. 802.15.4e, 2012.

[20] R. Niu, B. Chen, and P. Varshney, "Fusion of decisions transmitted over Rayleigh fading channels in wireless sensor networks," *IEEE Trans. Signal Process.*, vol. 54, no. 3, pp. 1018–1027, Mar. 2006.

[21] CHERRY. [Online]. Available: http://www.cherrycorp.com/english/_switches/energy%20harvesting/index.htm

[22] Mide Technology Corporation, Boston, MA, USA. [Online]. Available: http://www.mide.com/products/volture/piezoelectric-vibration-energy-harvesters.php

[23] B. Medepally, N. B. Mehta, and C. R. Murthy, "Implications of energy profile and storage on energy harvesting sensor link performance," in *Proc. IEEE GLOBECOM*, Dec. 2009, pp. 1695–1700.

[24] H. Nam, Y.-C. Ko, and M.-S. Alouini, "Spectral efficiency enhancement in multi-channel systems using redundant transmission and diversity reception," *IEEE Trans. Wireless Commun.*, vol. 7, no. 6, pp. 2143–2153, Jun. 2008.

[25] C.-H. Lim and J. Cioffi, "Performance of the adaptive rate MQAM with on/off power control," *IEEE Commun. Lett.*, vol. 5, no. 1, pp. 16–18, Jan. 2001.

[26] Y. Chen, Q. Zhao, V. Krishnamurthy, and D. Djonin, "Transmission scheduling for sensor network lifetime maximization: A shortest path bandit formulation," in *Proc. IEEE ICASSP*, May 2006, pp. IV:145–IV:149.

[27] R. Talak and N. B. Mehta, "Optimal timer-based best node selection for wireless systems with unknown number of nodes," *IEEE Trans. Commun.*, vol. 61, no. 11, pp. 4475–4485, Nov. 2013.

[28] X. Qin and R. Berry, "Opportunistic splitting algorithms for wireless networks," in *Proc. IEEE INFOCOM*, Mar. 2004, pp. 1662–1672.

[29] V. Shah, N. B. Mehta, and R. Yim, "Splitting algorithms for fast relay selection: Generalizations, analysis, and a unified view," *IEEE Trans. Wireless Commun.*, vol. 9, no. 4, pp. 1525–1535, Apr. 2010.

[30] D. Coppersmith and S. Winograd, "Matrix multiplication via arithmetic progressions," *J. Symb. Comput.*, vol. 9, no. 3, pp. 251–280, Mar. 1990.

Shilpa Rao received the B.Eng. degree in electronics and communication engineering from Sri Jayachamarajendra College Of Engineering, Mysore, India, in 2006. She is currently working toward the Ph.D. degree with the Department of Electrical Communication Engineering, Indian Institute of Science (IISc), Bangalore, India. From 2006 to 2009, she was with Toshiba Software (India) Pvt. Ltd., working on software development for video codecs. Her research interests include design and analysis of energy harvesting wireless sensor networks.

Neelesh B. Mehta (S'98–M'01–SM'06) received the B.Tech. degree in electronics and communications engineering from the Indian Institute of Technology (IIT), Madras, India, in 1996 and the M.S. and Ph.D. degrees in electrical engineering from the California Institute of Technology, Pasadena, CA, USA, in 1997 and 2001, respectively. He is currently an Associate Professor with the Department of Electrical Communication Engineering, Indian Institute of Science (IISc), Bangalore, India. Before joining IISc in 2007, he was a Research Scientist in the United States from 2001 to 2007 with AT&T Laboratories in New Jersey, Broadcom Corporation in New Jersey, and Mitsubishi Electric Research Laboratories in Massachusetts.

His research includes work on link adaptation, multiple-access protocols, cellular systems, MIMO, cooperative communications, energy harvesting networks, and cognitive radio. He was also actively involved in the Radio Access Network (RAN1) standardization activities in 3GPP from 2003 to 2007. He is an Editor of the IEEE Wireless Communications Letters and the IEEE Transactions on Communications and an Executive Editor of the IEEE Transactions on Wireless Communications. He served as the Director of Conference Publications on the Board of Governors of the IEEE ComSoc in 2012–13 and currently serves as a Member-at-Large on the Board.